國立交通大學

物理研究所

碩 士 論 文

磁化電漿中的尾波場

Wakefield In Magnetized Plasma

研 究 生 ： 張研俞 (Yen –Yu , Chang)

指導教授 ： 林貴林 (Prof. Lin – Guey , Lin)

中華民國九十七年七月

題目：磁化電漿中的尾波場

學生：張研俞　　指導教授：林貴林教授

國立交通大學物理碩士班

摘要

高能宇宙射線(UHECR)的來源，一直是天文物理所要探討的題目之一。其中利用太空中的電漿所產生之電場（尾波場），讓帶電粒子加速至極高能量，是可能的來源之一。

本篇論文主要呈現利用數值分析的方法，探討在均勻磁場下之電漿，受到強場電磁波激發後，所產生之尾波場的行為。

關鍵字：電漿，尾波場，天文粒子，電漿加速

Topic : Wakefield in Magnetized Plasma

Student : Yen – Yu, Chang Advisor : Prof. Lin – Guey, Lin

Institute of Physics

National Chiao Tung University

Abstract

The source of ultra high energy cosmic ray (UHECR) has been a mystery in astrophysics for years. It has been proposed that the plasma wakefield acceleration could be a possible acceleration mechanism for UHECR.

In this thesis, we present a numerical calculation of wakefield in the magnetized plasma, taking into account the relativistic effects.

Keywords : wakefield, plasma, plasma acceleration, UHECR

誌謝

首先，我要感謝一直在身後默默支持我的家人，尤其是爸爸、媽媽；你們的關心與鼓勵，是讓我前進的最大動力。

其次，感謝林教授不厭其煩的諄諄教誨，除了學術上的指導外，更讓我學習到作科學研究應有的觀念與態度。

最後，還要謝謝所有指導過我的師長、學長姐們、以及身邊的同學、朋友們。在碩士班的這兩年裡，我從大家身上學習到很多。

研俞　　07.23.2008

Contents

List of Figures

Chapter 1

Introduction

The source of ultra high energy cosmic ray (UHECR) is still a mystery. So far, the model for the source of UHECR can be divided into two categories, one is "top down"[1] scenario and the other is "bottom up"[2] scenario.

From results of several recent observations like HiRes [3] and Auger [4], the "ankle"in energy spectrum of cosmic rays exhibit the Greisen-Zatepin-Kuzmin suppression [5] [6] (Fig. 1.1). Hence the "bottom up"scenario seems more favorable than the "top down"scenario. Therefore, it is desirable to construct a theory for UHECR acceleration.

From the experience of terrestrial particle acceleration, one obtains important conditions for possible acceleration mechanism [8]: First, the trajectories of the accelerated charged particles should have no bending otherwise the effect of synchrotron radiation would reduce the energy of the particle. Second, the system should be collision free or else the energy of the accelerated particle would be transferred and spread out. To fulfill these conditions, plasma wakefield acceleration has been proposed as a possible mechanism for UHECR acceleration [7] [8].

When an EM wave packet injects into the plasma, the non-uniform electric field of the pulse imposes a longitudinal force (ponderomotive force) to electrons. Thus an electrostatic wave with phase velocity close to the group velocity of the driving pulse is excited behind this packet. We call this excited electric field as wakefield. When an electron has longitudinal velocity close to the phase velocity of this wave, it can be accelerated by this excited electric field [7] [10].

There are several methods to induce wakefield [10]. However, some of

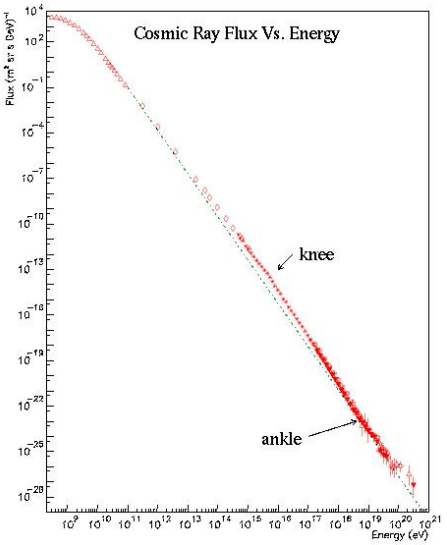

Figure 1.1: The energy spectrum of cosmic ray.

them are not available in the astrophysical settings. In astrophysical settings, the "magnetowave"induced wakefield seems more possible.

The simulation of magnetowave induced wakefield has been carried out [9]. However, the behavior of wakefield induced by a strong driven pulse is still unclear. Although we can derive theoretical approximation of wakefield in the weak field case (**Section 4.2**), it is difficult to extend this result to the strong field limit because relativistic dynamics makes the problem much more complicated. Therefore, we directly solve differential equations governing the wakefield by the numerical method.

Before jumping to the main theme of the thesis, we verify our numerical methods with well-studied cases.

In **Chapter 2**, we discuss the wakefield induced in **non-magnetized** plasma in the weak field case. We present the analytical derivation in **Section 2.2** [11]. Our numerical method is presented in **Section 2.3**. The comparison of analytical and numerical solution is given in **Section 2.4**.

In **Chapter 3**, we present the numerical method in **Section 3.2**. We then compare our result with previous works in **Section 3.3** [12].

In **Chapter 4**, we derive the wakefield induced by the whistler pulse [9]

in the weak field case, as presented in **Section 4.2**. We then verify this result by our numerical approach.

The main result of this thesis is presented in **Section 4.3** and **4.4**, which is the calculation of wakefield induced by right-handed circularly polarized pulse in arbitrary strength.

Chapter 5 is the conclusion.

Chapter 2

Wakefield in Non-Magnetized Plasma - Weak Field Case

2.1 Introduction

To make sure that our numerical method is reliable, we apply this method to several well-studied cases.

In this chapter, we present the analytical expression of plasma wakefield [11] in **Section 2.2** and demonstrate our numerical method in **Section 2.3**. The comparison of both approaches are presented in **Section 2.4**.

2.2 Analytical Solution

First of all, we consider the simplest case: an EM pulse with small amplitude sent into the plasma. In this limit, the electric field of the pulse is so small that velocities of the expelled electrons are much less than the speed of light. Therefore,we do not need to consider relativistic effects here. Furthermore, the plasma is not subject to any external field.

Following the above conditions, we shall derive the longitudinal electric field (wakefield) analytically in this section [11], and show the numerical result in the next section.

Lorentz force equation

The equation of motion of an electron in an electromagnetic field is

$$\frac{d\mathbf{P}}{dt} = -e(\mathbf{E} + (\mathbf{v} \times \mathbf{B})/c), \tag{2.1}$$

where $\mathbf{P}$ is the momentum of the electron, and $\mathbf{E}, \mathbf{B}$ are electric and magnetic field respectively.

Relating EM field to the scalar and vector potentials,

$$\begin{cases} \mathbf{E} = -\frac{1}{c}\frac{\partial \mathbf{A}}{\partial t} - \nabla\Phi, \\ \mathbf{B} = \nabla \times \mathbf{A} \end{cases} \tag{2.2}$$

we can rewrite the equation of motion as

$$\frac{d\mathbf{P}}{dt} = -e(-\frac{1}{c}\frac{\partial \mathbf{A}}{\partial t} - \nabla\Phi + (\mathbf{v} \times \nabla \times \mathbf{A})/c). \tag{2.3}$$

If the given pulse is propagating in z direction, we may assume that the scalar and vector potentials $(\Phi, \mathbf{A})$ are only a function of z and t. Therefore, the right hand side of equation (2.3) is just

$$\begin{aligned} &-e(-\frac{1}{c}\frac{\partial A_x}{\partial t} - \frac{v_z}{c}\frac{\partial A_x}{\partial z})\hat{\mathbf{e}}_x + \\ &-e(-\frac{1}{c}\frac{\partial A_y}{\partial t} - \frac{v_z}{c}\frac{\partial A_y}{\partial z})\hat{\mathbf{e}}_y + \\ &-e(-\frac{1}{c}\frac{\partial A_z}{\partial t} - \frac{\partial \Phi}{\partial z})\hat{\mathbf{e}}_z, \end{aligned} \tag{2.4}$$

here we expend the vector form to three components. Focusing on x and y components, we have

$$\frac{d\mathbf{p}}{dt} = -(-\frac{\partial \mathbf{a}}{\partial t} - v_z\frac{\partial \mathbf{a}}{\partial z}), \tag{2.5}$$

where $\mathbf{a} = (a_x, a_y) = e(A_x, A_y)/mc^2$ is the normalized vector potential and $\mathbf{p} = (p_x, p_y) = (P_x, P_y)/mc$ is the normalized momentum. We note that

$$\frac{d}{dt} = \frac{\partial}{\partial t} + \mathbf{v} \cdot \nabla, \tag{2.6}$$

which means

$$\frac{d\mathbf{a}}{dt} = \frac{\partial \mathbf{a}}{\partial t} + \mathbf{v} \cdot \nabla\mathbf{a}. \tag{2.7}$$

Since $\mathbf{a}$ is function of z and t only, the above could be rewritten as

$$\frac{d\mathbf{a}}{dt} = \frac{\partial \mathbf{a}}{\partial t} + v_z\frac{\partial \mathbf{a}}{\partial z}. \tag{2.8}$$

Therefore, equation (2.7) becomes

$$\frac{d\mathbf{p}}{dt} = \frac{d\mathbf{a}}{dt}, \tag{2.9}$$

which implies

$$\mathbf{p} = \mathbf{a} + C_0. \tag{2.10}$$

At $(z,t) = (0,0)$, $\mathbf{a}$ is zero, hence $\mathbf{p} = C_0$. However, the momentum of the electron should be zero since we are considering the cold plasma. Therefore, $C_0 = 0$. Thus we have $\mathbf{p} = \mathbf{a}$.

Concerning the z-component of equation (2.3), we have

$$\begin{aligned} \frac{dP_z}{dt} &= -e(E_z + (v_x B_y - v_y B_x)/c) \\ &= -e(-\frac{\partial \Phi}{\partial z} + (v_x(\frac{\partial A_x}{\partial z}) + v_y(\frac{\partial A_y}{\partial z}))/c). \end{aligned} \tag{2.11}$$

Since $(v_x, v_y) = e(A_x, A_y)/mc$ by equation (2.10), we can rewrite the above equation as

$$\begin{aligned} \frac{dP_z}{dt} &= -e(-\frac{\partial \Phi}{\partial z} + \frac{e}{mc^2}(A_x(\frac{\partial A_x}{\partial z}) + A_y(\frac{\partial A_y}{\partial z}))) \\ &= -e(-\frac{\partial \Phi}{\partial z} + \frac{mc^2}{2e}(\frac{\partial |\mathbf{a}|^2}{\partial z})) \end{aligned} . \tag{2.12}$$

Since we are dealing with non-relativistic motion, we have $p_z = mv_z$. With $d/dt = \partial/\partial t + v_z \partial/\partial z$ we rewrite equation (2.12) as

$$\frac{\partial \beta_z}{\partial t} + v_z \frac{\partial \beta_z}{\partial z} = (\frac{\partial \phi}{\partial z} - \frac{1}{2}\frac{\partial |\mathbf{a}|^2}{\partial z}), \tag{2.13}$$

where $\phi = e\Phi/mc^2$ and $\beta_z = v_z/c$.

Continuity equation

Knowing how electrons are affected by the EM pulse, we further study the collective effect on plasma.

In the following derivation, we consider only two species of particles in the plasma: electrons and ions. Since ions are much heavier than electrons, we assume ions are almost motionless in comparison with electrons. Thus we ignore the dynamics of ions.

Furthermore, we assume collisions between particles can be neglected, thus there are no abrupt change for the path of moving particles. Therefore, the total number of particles in unit volume should conserve. In other words, the number density of electrons obey the continuity equation given by

$$\frac{dn}{dt} = \frac{\partial n}{\partial t} + \nabla \cdot (n\mathbf{v}) = 0, \tag{2.14}$$

where n is the number density of the electrons and $\mathbf{v}$ is the velocity of electrons.

Let us denote the electron density n as $n = (n_0 + \delta n)$, where n_0 is the density in the equilibrium state(the density when the electrons are not perturbed) and δn is the perturbation. By replacing n with $(n_0 + \delta n)$ and ignoring the quadratic terms in perturbations, the continuity equation becomes

$$\frac{\partial \delta n}{\partial t} + n_0 \nabla \cdot \mathbf{v} = 0. \tag{2.15}$$

Again we only consider the case where $\mathbf{v}$ is a function of (z, t) ($\mathbf{v} \equiv \mathbf{v}(z, t)$). Therefore, the continuity equation becomes

$$\frac{\partial \delta n}{c\partial t} + n_0 \frac{\partial \beta_z}{\partial z} = 0, \tag{2.16}$$

where $\beta_z = v_z/c$.

Poisson equation

The electrostatic potential in the plasma is governed by the Poisson equation

$$\nabla^2 \Phi = 4\pi e(n - n_0). \tag{2.17}$$

Again we assume $\Phi = \Phi(z, t)$ and take $\phi = e\Phi/m_e c^2$. This leads to

$$\frac{\partial^2 \phi}{\partial z^2} = \frac{w_p^2}{c^2 n_0}(n - n_0), \tag{2.18}$$

where $w_p = \sqrt{4\pi e^2 n_0/m_e}$ is the plasma frequency.

Let us now return to equation (2.13). In the current limit, one may ignore the term $v_z \partial \beta_z/\partial z$. Taking one more derivative, $\partial/\partial z$, on both sides of this equation, we obtain

$$\frac{\partial^2 \beta_z}{c\partial z \partial t} = (\frac{\partial^2 \phi}{\partial z^2} - \frac{1}{2}\frac{\partial^2 |\mathbf{a}|^2}{\partial z^2}). \tag{2.19}$$

In this equation, we can replace $\partial^2\phi/\partial z^2$ by $w_p^2(n - n_0)/c^2 n_0$ from equation (2.18), and replace $\partial^2 \beta_z/\partial z \partial t$ by $-\partial^2 \delta n/cn_0 \partial t^2$, which can be derived from equation (2.16). We then arrive at the following equations for the plasma oscillation

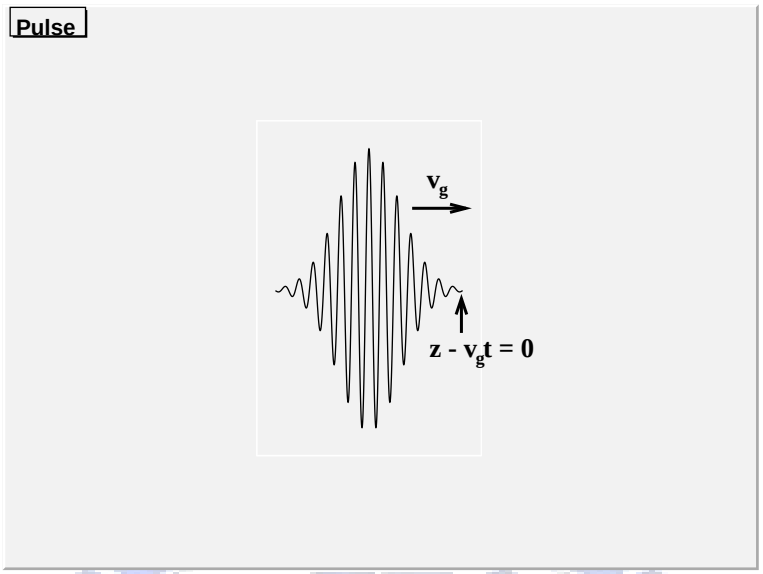

Figure 2.1: The plot of the pulse. We set the pulse moving toward positive z direction with speed v_g, the group velocity. Since we send the pulse into the system at $z = 0$ and $t = 0$, the position of the front point of the pulse is always zero in the co-moving frame [12].

$$\frac{\partial^2 \delta n}{\partial t^2} + w_p^2 \delta n = \frac{n_0 c^2}{2} \frac{\partial^2 |\mathbf{a}|^2}{\partial z^2}. \tag{2.20}$$

For convenience, we change the coordinate to the co-moving frame (Fig. 2.1) with the pulse, $\xi = \frac{\omega_p}{c}(z - v_g t)$, where v_g is the group velocity of the pulse in the plasma. Then the above equation can be recasted into

$$\frac{\partial^2 \widetilde{\delta n}}{\partial \xi^2} + \widetilde{\delta n} = \frac{c^2}{2v_g^2} \frac{\partial^2 |\mathbf{a}|^2}{\partial \xi^2}, \tag{2.21}$$

where $\widetilde{\delta n} = \delta n / n_0$.

We note that equation (2.21) appears as an equation of oscillation, and the term $\mathbf{a}$ on the right hand side is determined by the pulse.

Analytical solution

Solving equation (2.21), we obtain

$$\widetilde{\delta n}(\xi) = \frac{c^2}{2v_g^2}(|\mathbf{a}(\xi)|^2 - \int_{\infty}^{\xi} |\mathbf{a}(\xi')|^2 \sin(\xi - \xi') d\xi'), \tag{2.22}$$

under the boundary condition that $\mathbf{a} = 0$ for $\xi \to \infty$. Using

$$\nabla \cdot \mathbf{E} = -4\pi e \delta n, \tag{2.23}$$

and assuming that the electric field $\mathbf{E}$ is only a function of (z, t), we obtain

$$\frac{\partial E_z}{\partial z} = -4\pi e \delta n. \tag{2.24}$$

Changing the coordinate and normalizing all the quantities, we have

$$\frac{\partial \widetilde{E_z}}{\partial \xi} = -\widetilde{\delta n}, \tag{2.25}$$

where $\widetilde{E_z} = eE_z/m_e c\omega_p$. Finally, by combining equation (2.22) and (2.25), we obtain the wakefield $\widetilde{E_z}$:

$$\begin{aligned} \widetilde{E_z} &= -\int \widetilde{\delta n} d\xi' \\ &= -\frac{c^2}{2v_g^2} \int (|\mathbf{a}(\xi')|^2 - \int_\infty^{\xi'} |\mathbf{a}(\xi'')|^2 \sin(\xi' - \xi'') d\xi'') d\xi'. \end{aligned} \tag{2.26}$$

2.3 Numerical Method

Linearly polarized pulse

For convenience, we assume the pulse is linearly polarized in $\hat{x}$ direction and propagating toward positive $\hat{z}$ direction. First of all, the equations of motion for electrons are

$$\begin{cases} m\frac{dv_x}{dt} = -e(E_x + \frac{1}{c}(v_y B_z - v_z B_y)), \\ m\frac{dv_y}{dt} = -e(E_y + \frac{1}{c}(v_z B_x - v_x B_z)), \\ m\frac{dv_z}{dt} = -e(E_z + \frac{1}{c}(v_x B_y - v_y B_x)). \end{cases} \tag{2.27}$$

Since, E_y, B_x and B_z vanish here, the second equation is trivial and we need only consider the first and third equations. Setting the pulse as $\mathbf{E}(z, t) = E_0 \cos(kz - \omega t)\hat{\mathbf{e}}_x$, we have

$$m\frac{dv_x}{dt} = -eE_0(1 - \frac{v_z}{c})(\cos(kz - \omega t)), \tag{2.28}$$

$$m\frac{dv_z}{dt} = -e(E_z + E_0(\frac{v_x}{c}\cos(kz - \omega t)). \tag{2.29}$$

Again, we need to consider the collective effect of plasma as in the last section. Therefore, we apply the continuity equation as before (equation (2.16))

$$\frac{\partial \delta n}{c\partial t} + n_0 \frac{\partial \beta_z}{\partial z} = 0. \tag{2.30}$$

Also, we apply the Gauss law for the electric field

$$\frac{\partial E_z}{\partial z} = -4\pi e(n - n_0). \tag{2.31}$$

Applying partial derivative on t to equation (2.31) and combining with equation (2.30), we obtain

$$\frac{\partial^2 E_z}{\partial t \partial z} = -4\pi e n_0 \frac{\partial v_z}{\partial z}. \tag{2.32}$$

Now we have three differential equations (2.28), (2.29), (2.32) and three unknown quantities v_x, v_z, E_z, where E_z is the wakefield to be determined.

Focusing on equations (2.28) and (2.29), we rewrite the time derivative $d/dt = \partial/\partial t + v_z \partial/\partial z$ on the left hand side

$$\begin{aligned} m\frac{dv_x}{dt} &= m(\frac{\partial v_x}{\partial t} + v_z \frac{\partial v_x}{\partial z}), \\ m\frac{dv_z}{dt} &= m(\frac{\partial v_z}{\partial t} + v_z \frac{\partial v_z}{\partial z}). \end{aligned} \tag{2.33}$$

Changing the coordinate to the co-moving frame of the pulse $\xi = \frac{\omega_p}{c}(z - v_g t)$ as before, equations (2.28) and (2.29) are recasted into

$$\begin{aligned} m(-\omega_p \frac{\partial v_x}{\partial \xi} + k_p v_z \frac{\partial v_x}{\partial \xi}) &= -eE_0(1 - \beta_z)(\cos(\widetilde{k}\xi)), \\ m(-\omega_p \frac{\partial v_z}{\partial \xi} + k_p v_z \frac{\partial v_z}{\partial \xi}) &= -e(E_z + E_0 \beta_x \cos(\widetilde{k}\xi)), \end{aligned} \tag{2.34}$$

where β_x, β_z and $\widetilde{k}$ equal to $v_x/c, v_z/c$ and kc/ω_p respectively. Taking $\widetilde{E} = eE/m_e c\omega_p$ as the normalized electric field, we finally obtain

$$\begin{aligned} -\frac{v_g \partial \beta_x}{c\partial \xi} + \beta_z \frac{\partial \beta_x}{\partial \xi} &= -\widetilde{E}_0(1 - \beta_z)\cos(\widetilde{k}\xi), \\ -\frac{v_g \partial \beta_z}{c\partial \xi} + \beta_z \frac{\partial \beta_Z}{\partial \xi} &= -\widetilde{E}_z - \widetilde{E}_0 \beta_x (\cos(\widetilde{k}\xi)). \end{aligned} \tag{2.35}$$

With the new variables, equation (2.32) is converted into

$$\frac{\partial^2 E_z}{\partial \xi^2} = -\frac{v_g \partial \beta_z}{c\partial \xi}, \tag{2.36}$$

or

$$\frac{\partial E_z}{\partial \xi} = -\beta_g \beta_z, \tag{2.37}$$

where $\beta_g = v_g/c$. Combining equation (2.35) and (2.37), we are now ready to solve the plasma wakefield numerically.

Boundary conditions

Since we assume the plasma is cold, the wakefield and the velocities of electrons are zero for $\xi \to \infty$. Thus the boundary conditions for various quantities are: $\vec{\beta} = 0$ and $\tilde{E}_z = 0$ for $\xi \to \infty$.

2.4 Comparison

In this section, we compare results of **Sections (2.2)** and **(2.3)**.

Gaussian pulse

Originally, the input pulse is

$$\mathbf{E}(z,t) = \hat{x} E_M \int_{-\infty}^{\infty} \mathbf{e}^{-(k-k_0)^2/2\mu^2} \mathbf{e}^{i(kz-\omega(k)t)} dk, \tag{2.38}$$

where E_M is the maximum amplitude of the pulse, and k_0 is the average wave number of the pulse and $\omega(k)$ is the frequency of the pulse given by the dispersion relation

$$\omega^2 = k^2 c^2 + \omega_p^2. \tag{2.39}$$

For $k^2c^2 >> \omega_p^2$, the phase velocity and group velocity are approximately equal to c. That is,

$$\frac{\omega}{k} \simeq \frac{d\omega}{dk} = v_g \simeq c. \tag{2.40}$$

Therefore, we have $kz - \omega(k)t = k(z - v_g t) = \tilde{k}\xi$. Thus equation (2.38) becomes

$$\mathbf{E}(\xi) = \hat{x} E_M \int_{-\infty}^{\infty} \mathbf{e}^{-(k-k_0)^2/2\mu^2} \mathbf{e}^{i\tilde{k}\xi} dk. \tag{2.41}$$

In our calculation, we do not integrate the Fourier transform but simply set the Gaussian pulse as

$$\mathbf{E}(\xi) = \hat{x} E_M \mathbf{e}^{-(\xi-\xi_0)^2/2\sigma^2} \cos(\tilde{k}\xi). \tag{2.42}$$

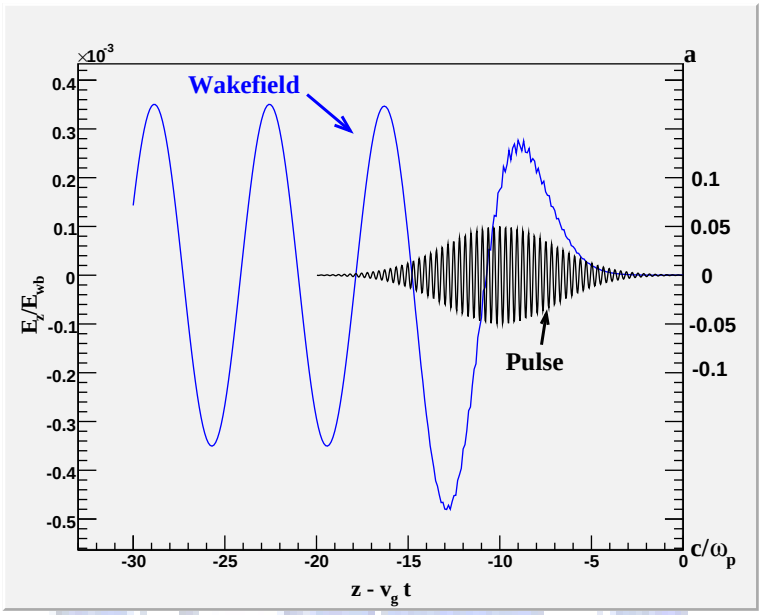

Figure 2.2: This is the plot of wakefield, where $E_{wb} = mc\omega_p/e$ is the normalization factor and $a = eE/mc\omega$. The x-axis represents the co-moving frame where the unit length is c/ω_p. The amplitude of the pulse is $a_0 = 0.05$, the wave number is $\tilde{k} = 20$ and $\sigma = 3c/\omega_p$.

Result

Here we introduce two important parameters. One is called the "strength parameter", defined as

$$a_0 = \frac{eE_M}{mc\omega} \tag{2.43}$$

is the normalized factor for the pulse. The other parameter is called the "cold wavebreaking field"[7], defined as

$$E_{wb} = \frac{eE}{mc\omega_p} \tag{2.44}$$

is the normalized factor for the wakefiled. The reason we use this normalization is that the maximum amplitude which the plasma wakefield can support is $E_{Max} \simeq a_0 E_{wb}$ [8].

Setting $a_0 = 0.05$, $\tilde{k} = ck/\omega_p = 20$ and $\sigma = 3c/\omega_p$, we present the wakefield in Fig. 2.2. One can see that the wakefield behave smoothly in ξ.

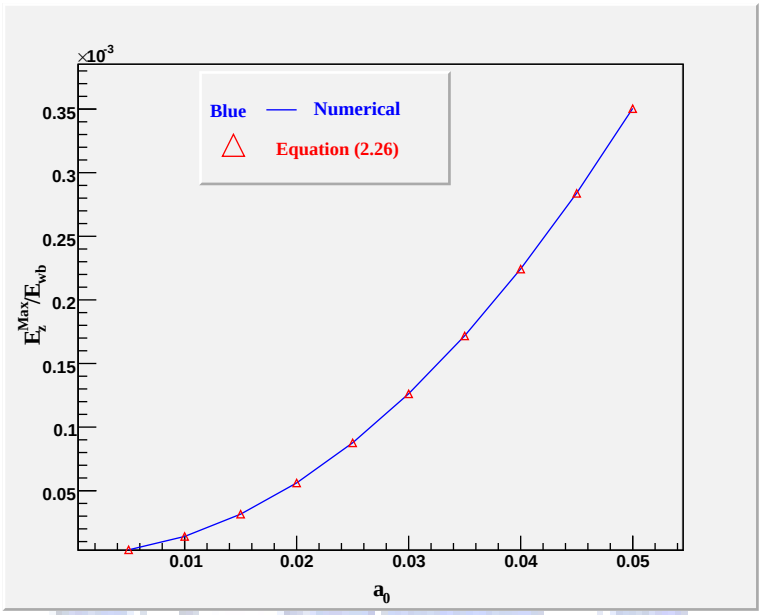

Figure 2.3: The comparison of wakefield obtained numerically and analytically.

In Fig. 2.3, we varying the maximum amplitude of the pulse and taking the maximum value of wakefield. One can see the wakefield obtained numerically agrees very well with the analytical result. From equation (2.26), one can see that $E_z^{Max} \propto a_0^2$. This is also seen in Fig. 2.3.

Chapter 3

Wakefield in Non-Magnetized Plasma - Strong Field Case

3.1 Introduction

After checking how the numerical methods work in the weak field case, we consider strong field case. When the amplitude of the pulse becomes stronger, the speeds of driven electrons would be close to the speed of light. Thus the relativistic effect ($\mathbf{P} = \gamma m\mathbf{v}$) shall be taken into consideration.

In **Section 3.2**, we demonstrate how we derive and solve the system of differential equations which are the equations of motion for electrons, the continuity equation and the Poisson equation. Since wakefield in non-magnetized plasma with relativistic effects have been well studied [12], we use these results to check the numerical method. One can find the comparison in **Section 3.3**.

3.2 Numerical Solution

By increasing the amplitude of the pulse, the speed of the driven electron also increase. When the speed of electron is close to c, the speed of light, one has to consider the **relativistic dynamics** for solving the equation of motion for the electron.

γ factor

To derive the Lorentz force equation, we start from $d\mathbf{P}/dt$. Here the momentum $\mathbf{P}$ is no longer $m\mathbf{v}$ but $\gamma m\mathbf{v}$ with $\gamma = 1/\sqrt{1 - |\mathbf{v}|^2/c^2}$. Therefore,

the Lorentz force equation should be modified as

$$\frac{d\mathbf{P}}{dt} = \frac{m\mathbf{v}d\gamma}{dt} + \frac{\gamma m d\mathbf{v}}{dt} = -e(\mathbf{E} + (\mathbf{v} \times \mathbf{B})/c), \tag{3.1}$$

since γ is also a function of time.

Furthermore, since the kinetic energy of the electrons is given by

$$E_k = (\gamma - 1)mc^2, \tag{3.2}$$

we have

$$\frac{dE_k}{dt} = \frac{d\gamma}{dt}mc^2. \tag{3.3}$$

The left hand side of this equation is just the increasing rate of the electron kinetic energy, which is obviously $-e\mathbf{v} \cdot \mathbf{E}$. Therefore, we have

$$\frac{d\gamma}{dt} = \frac{-e\mathbf{v} \cdot \mathbf{E}}{mc^2}. \tag{3.4}$$

Rewriting $d\gamma/dt$ in equation (3.1), we arrive at

$$\frac{-e(\mathbf{v} \cdot \mathbf{E})m\mathbf{v}}{mc^2} + \frac{\gamma m d\mathbf{v}}{dt} = -e(\mathbf{E} + (\mathbf{v} \times \mathbf{B})/c). \tag{3.5}$$

Changing to the co-moving frame variable ξ and normalizing all quantities as before, we have

$$\begin{cases} -(\widetilde{\mathbf{E}} \cdot \vec{\beta})\beta_x + \gamma(-\beta_g \dfrac{\partial \beta_x}{\partial \xi} + \beta_z \dfrac{\partial \beta_x}{\partial \xi}) = -(\widetilde{E_x} + \beta_y \widetilde{B_z} - \beta_z \widetilde{B_y}), \\ -(\widetilde{\mathbf{E}} \cdot \vec{\beta})\beta_y + \gamma(-\beta_g \dfrac{\partial \beta_y}{\partial \xi} + \beta_z \dfrac{\partial \beta_y}{\partial \xi}) = -(\widetilde{E_y} + \beta_z \widetilde{B_x} - \beta_x \widetilde{B_z}), \\ -(\widetilde{\mathbf{E}} \cdot \vec{\beta})\beta_z + \gamma(-\beta_g \dfrac{\partial \beta_z}{\partial \xi} + \beta_z \dfrac{\partial \beta_z}{\partial \xi}) = -(\widetilde{E_z} + \beta_x \widetilde{B_y} - \beta_y \widetilde{B_x}), \end{cases} \tag{3.6}$$

where $\vec{\beta} = \mathbf{v}/c$ and $\beta_g = v_g/c$.
The continuity equation (2.14)

$$\frac{\partial n}{\partial t} + \nabla \cdot (n\mathbf{v}) = 0 \tag{3.7}$$

can be written as

$$-\beta_g \frac{\partial \widetilde{n}}{\partial \xi} + \frac{\partial(\widetilde{n}\beta_z)}{\partial \xi} = 0, \tag{3.8}$$

where $\widetilde{n} = n/n_0$.

Finally the Poisson equation can be written as

$$-\frac{\partial \widetilde{E_z}}{\partial z} = \frac{\omega_p}{c}(\widetilde{n} - 1), \tag{3.9}$$

or

$$-\frac{\partial \widetilde{E_z}}{\partial \xi} = (\widetilde{n} - 1). \tag{3.10}$$

Combining equations (3.6), (3.8) and (3.10), we have five equations and five unknown quantities $\beta_x, \beta_y, \beta_z, \widetilde{n}$ and $\widetilde{E_z}$. We can solve the system of differential equations to find E_z.

Boundary conditions

Again we take the wakefield and velocities of electrons as zero for $\xi \to \infty$. Furthermore, we have $\tilde{n} = 1$ for $\xi \to \infty$.

3.3 Verifying Numerical Methods

The solution of wakefield including relativistic effect is well-studied. Here we refer to the result by Sprangle, Esarey and Ting [12] and compare our calculation with their results . For simplicity, we just show their equations and present the solution. One can find the derivation of equation in **Appendix A**. The equation they derived (see Appendix A) is

$$\frac{\partial^2 \phi}{\partial \xi^2} = \frac{1}{2}(\frac{1 + |\mathbf{a}|^2}{(1+\phi)^2} - 1), \tag{3.11}$$

where $|\mathbf{a}|^2$ and ϕ is defined in equations (2.5) and (2.13) respectively.

The term $\mathbf{a}$ is determined by the given pulse, and the wakefield to be determined is $\widetilde{E_z} = -\partial\phi/\partial\xi$. Let $\widetilde{E_z}$ have a maximum value at ξ_0, then

$$\frac{\partial \widetilde{E_z}}{\partial \xi}|_{\xi=\xi_0} = -\frac{\partial^2 \phi}{\partial \xi^2}|_{\xi=\xi_0} = 0, \tag{3.12}$$

which implies that

$$\frac{1 + |\mathbf{a}|^2}{(1+\phi)^2} - 1|_{\xi=\xi_0} = 0. \tag{3.13}$$

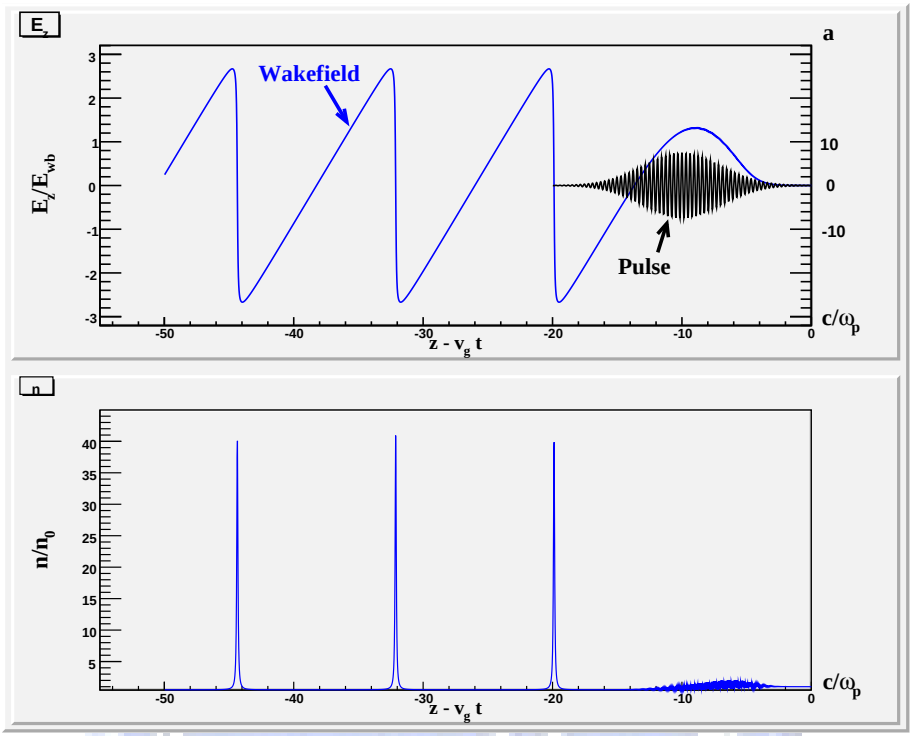

Figure 3.1: The plot of wakefield and normalized density in the co-moving frame, where we set $a_0 = 7.5$, $\tilde{k} = 40$ and $\sigma = 3c/\omega_p$.

Hence [15]

$$\widetilde{E_z}^{Max} \propto \frac{a_0^2}{\sqrt{a_0^2 + 1}} \tag{3.14}$$

which implies $\widetilde{E_z}^{Max}$ is proportional to a_0 for $a_0 >> 1$.

Result

Setting $a_0 = 7.5$, $\tilde{k} = 40$ and $\sigma = 3c/\omega_p$, one can see the wakefield in Fig. 3.1. When the pulse amplitude increases, the ponderomotive force acts on the driven electrons becomes larger. Thus the longitudinal momentum of the driven electrons become larger, too. Such large longitudinal momentum allows electrons to "squeeze"in small region while oscillating (Fig. 3.1). Therefore, the electric field would goes down sharply during the crowds of electrons. Hence the behavior of the wakefield is no longer sinusoidal but saw-tooth-like.

In Fig. 3.2, we compare the results from two different methods. One can see that the numerical solution agrees well with the solution of equation

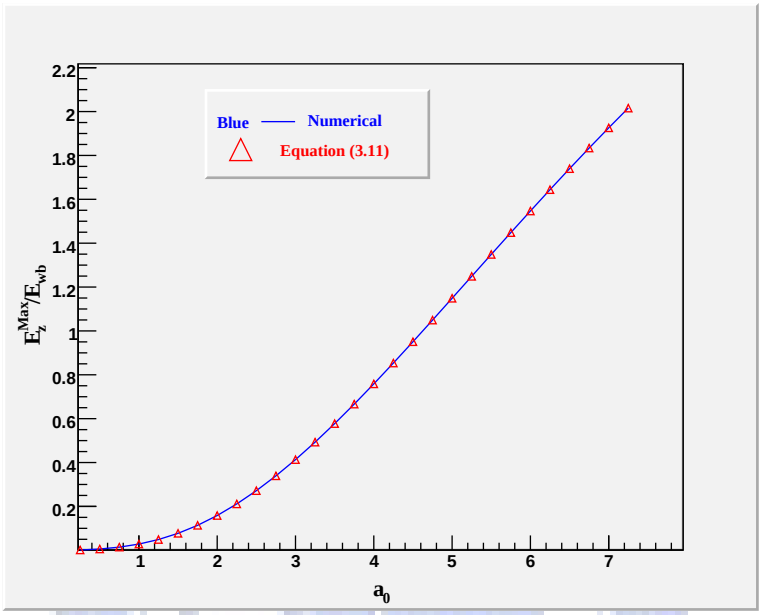

Figure 3.2: The plot of maximum wakefield versus pulse amplitude. The settings of the driving pulse are $\tilde{k} = 40$ and $\sigma = 3\sqrt{2}c/\omega_p$.

(3.11). We can also see that $\widetilde{E_z} \propto a_0$ when $a_0 >> 1$.

Chapter 4

Wakefield in Magnetized Plasma

4.1 Introduction

In this chapter, we will present our main result : the wakefield induced by right-handed circularly polarized pulse in the magnetized plasma. The strength of the pulse will be taken as arbitrary.

In the magnetized plasma, there are four modes of EM waves. Here we focus on the right-handed circularly polarized wave, which is described by the dispersion relation

$$k^2c^2 - \omega^2 + \frac{\omega\omega_p^2}{\omega - \omega_c} = 0 \tag{4.1}$$

in the non-relativistic limit where $\omega_c = eB/mc$ is the cyclotron frequency. There are two solutions to this dispersion equation (Fig. 4.1), one is called R wave (the upper branch) and the other is called whistler wave (the lower branch).

Since the ponderomotive force in the magnetized plasma in the non-relativistic limit has been well studied [13], we can use this result to derive analytical approximation of wakefield in this case. Furthermore, we can use this approximation to check the numerical method in the non-relativistic limit. The derivation of the analytical approximation is given in **Section 4.2**.

In **Section 4.3**, we analyze the wakefield induced by the whistler pulse. We compare numerical solutions with analytical approximation (Fig. 4.2).

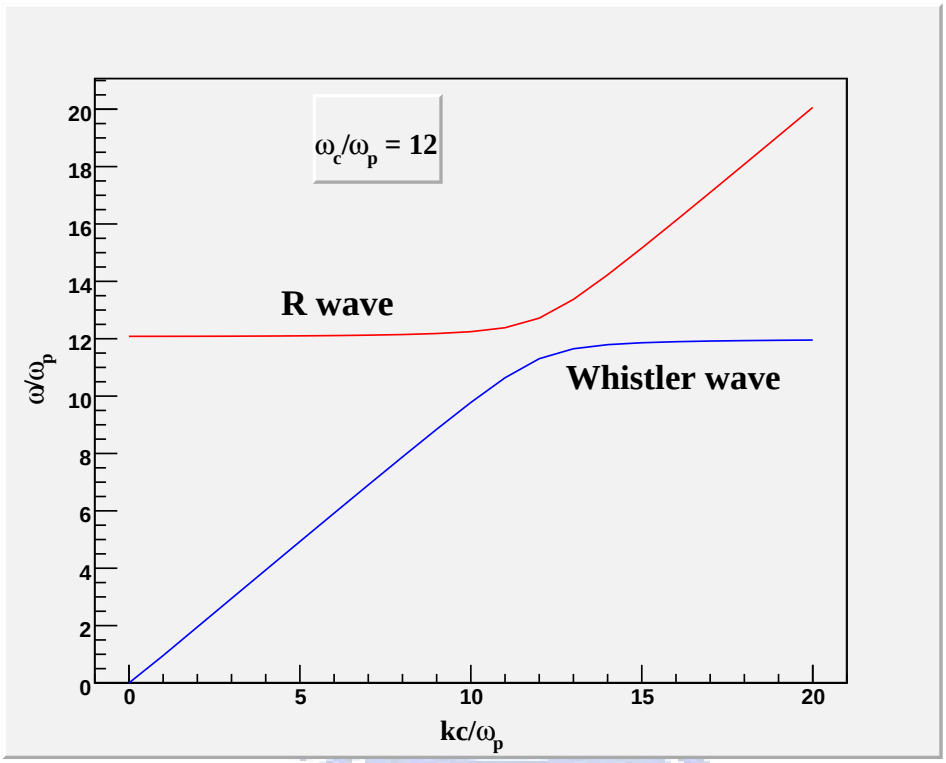

Figure 4.1: The plot of dispersion relation of right-handed circularly polarized EM wave in the magnetized plasma without considering relativistic effects. The upper branch is called R wave while the lower branch is called whistler wave.

Since there exist simulation results (Particle In Cell simulation) of wakefield in the magnetized plasma [9], we also compare our numerical solutions with the simulation results. Furthermore, we will consider the case of strong whistler pulse and calculate the wakefield.

In **Section 4.4**, we take the driving pulse as the R wave with arbitrary amplitude and analyze γ factors of the driven electrons and the wakefield .

4.2 The Analytical Solutions in Weak Field Case

In chapters 2 and 3, we dealt with unmagnetized plasma. However, in many physical systems, the external magnetic field should be taken into consideration. Here we focus on the particular situation that a circularly polarized EM pulse is propagating along the external magnetic field direction. For convenience, this direction is taken to be the z-axis.

Derivation of wakefield

To derive the wakefield, let us first rewrite the z component of Lorentz force,

$$\frac{dP_z}{dt} = -e(E_z + \frac{1}{c}(v_x B_y - v_y B_x)). \tag{4.2}$$

In the non-relativistic limit, we can approximate the last term on the right hand side by $f_\parallel$ (see Appendix B). That is, we have

$$\frac{-e}{c}(v_x B_y - v_y B_x) = f_\parallel, \tag{4.3}$$

where

$$f_\parallel = \frac{-1}{2}(\frac{\partial}{\partial z} - \frac{k\omega_c}{\omega(\omega-\omega_c)}\frac{\partial}{\partial t})\frac{e^2 E_0^2}{m\omega(\omega-\omega_c)}, \tag{4.4}$$

where k and ω are the wave number and angular frequency of the pulse respectively, $\omega_c = eB_0/m_e c$ is the cyclotron frequency of the electron, and E_0 is the electric field amplitude of the pulse. Thus equation (4.4) can be written as

$$\frac{dP_z}{dt} = -eE_z + f_\parallel. \tag{4.5}$$

Noting that

$$\frac{dP_z}{dt} = \frac{\partial P_z}{\partial t} + v_z\frac{\partial P_z}{\partial z}, \tag{4.6}$$

and assuming that the quadratic term (the last term in the right hand side) is negligible in the non-relativistic limit, equation (4.5) can be written as

$$m\frac{\partial v_z}{\partial t} = -eE_z + f_{\parallel}, \tag{4.7}$$

where we just replace P_z by mv_z.

Equations (2.16) and (2.18) are still valid in this case.

$$\frac{\partial n}{\partial t} + n_0\frac{\partial v_z}{\partial z} = 0, \tag{4.8}$$

$$\frac{\partial^2 \Phi}{\partial z^2} = 4\pi e(n - n_0). \tag{4.9}$$

Since $\partial\Phi/\partial z = -E_z$, equation (4.9) becomes

$$-\frac{\partial E_z}{\partial z} = 4\pi e(n - n_0). \tag{4.10}$$

Taking $\partial/\partial t$ on both sides of equation (4.10), we have

$$\frac{\partial^2 n}{\partial t^2} + n_0\frac{\partial^2 v_z}{\partial t \partial z} = 0. \tag{4.11}$$

Also, by taking $\partial/\partial z$ on both sides of equation (4.9), we arrive at

$$m\frac{\partial^2 v_z}{\partial z \partial t} = -e\frac{\partial E_z}{\partial z} + \frac{\partial f_{\parallel}}{\partial z}. \tag{4.12}$$

Combining equations (4.13) and (4.14), we acquire

$$-\frac{m}{n_0}\frac{\partial^2 n}{\partial t^2} = -e\frac{\partial E_z}{\partial z} + \frac{\partial f_{\parallel}}{\partial z}. \tag{4.13}$$

Furthermore, we can operate $\partial^2/\partial t^2$ on both sides of equation (4.10), which gives

$$-\frac{\partial^3 E_z}{\partial t^2 \partial z} = 4\pi e\frac{\partial^2 n}{\partial t^2}. \tag{4.14}$$

Finally, combining equations (4.13) and (4.14), we obtain

$$\frac{m}{4\pi e n_0}\frac{\partial^3 E_z}{\partial t^2 \partial z} = -e\frac{\partial E_z}{\partial z} + \frac{\partial f_{\parallel}}{\partial z}, \tag{4.15}$$

which is the differential equation for E_z.

Solution

Changing the variables (z,t) to $\xi = \frac{\omega_p}{c}(z - v_g t)$, equation (4.15) becomes

$$\begin{aligned}(\frac{\partial^2}{\partial\xi^2}+1)\frac{\partial E_z}{\partial\xi} &= \frac{1}{e}\frac{\partial f_\parallel}{\partial\xi} \\ &= -\frac{1}{2}\frac{\partial}{\partial\xi}(\frac{\omega_p}{c}\frac{\partial}{\partial\xi}+\frac{k\omega_c\omega_p}{\omega(\omega-\omega_c)}\frac{\partial}{\partial\xi})\frac{eE_0^2}{m\omega(\omega-\omega_c)} \\ &= -\frac{1}{2}(\frac{\omega_p}{c}+\frac{k\omega_c\omega_p}{\omega(\omega-\omega_c)})\frac{e}{m\omega(\omega-\omega_c)}\frac{\partial^2 E_0^2}{\partial\xi^2},\end{aligned} \tag{4.16}$$

where $f_\parallel$ is given by equation (4.6). Finally, E_z is solved as

$$\widetilde{E}_z(\xi) = \frac{-1}{2}(\frac{c}{v_g}+\frac{\tilde{\omega}_c}{\tilde{\omega}(\tilde{\omega}-\tilde{\omega}_c)})\frac{1}{\tilde{\omega}(\tilde{\omega}-\tilde{\omega}_c)}\int_\xi^\infty d\xi' \widetilde{E}_0^2(\xi')\cos(\xi-\xi'), \tag{4.17}$$

where $\widetilde{E} = eE/mc\omega_p$, $\tilde{\omega} = \omega/\omega_p$ and $\tilde{\omega}_c = \omega_c/\omega_p$. We can further simplify the solution to

$$\widetilde{E}_z(\xi) = \chi(\xi)(\frac{c}{v_g}+\frac{\tilde{\omega}_c}{\tilde{\omega}(\tilde{\omega}-\tilde{\omega}_c)})\frac{1}{\tilde{\omega}(\tilde{\omega}-\tilde{\omega}_c)}\widetilde{E}_M^2, \tag{4.18}$$

where E_M is the maximum amplitude of the pulse, and

$$\chi(\xi) = \frac{-1}{2}\frac{1}{\widetilde{E}_M^2}\int_\xi^\infty d\xi' \widetilde{E}^2(\xi')\cos(\xi-\xi'). \tag{4.19}$$

4.3 Numerical Solution of Wakefield Induced by Whistler Wave

In the following sections, we do not restrict ourselves in the small field limit. It is obvious that as the amplitude of the pulse increases, the motions of the affected electrons might be relativistic. Hence the solution in the last section might not be correct if the amplitude of the pulse is large.

We will show the numerical results by solving differential equations derived in **chapter 3** (equation (3.6), (3.8), (3.10)).

$$\begin{cases} -(\widetilde{\mathbf{E}}\cdot\vec{\beta})\vec{\beta}+\gamma(-\beta_g\frac{\partial\vec{\beta}}{\partial\xi}+\beta_z\frac{\partial\vec{\beta}}{\partial\xi}) = -(\widetilde{\mathbf{E}}+\vec{\beta}\times\widetilde{\mathbf{B}}), \\ -\beta_g\frac{\partial\widetilde{n}}{\partial\xi}+\frac{\partial(\widetilde{n}\beta_z)}{\partial\xi} = 0, \\ -\frac{\partial\widetilde{E_z}}{\partial\xi} = \beta_g^2(\widetilde{n}-1). \end{cases} \tag{4.20}$$

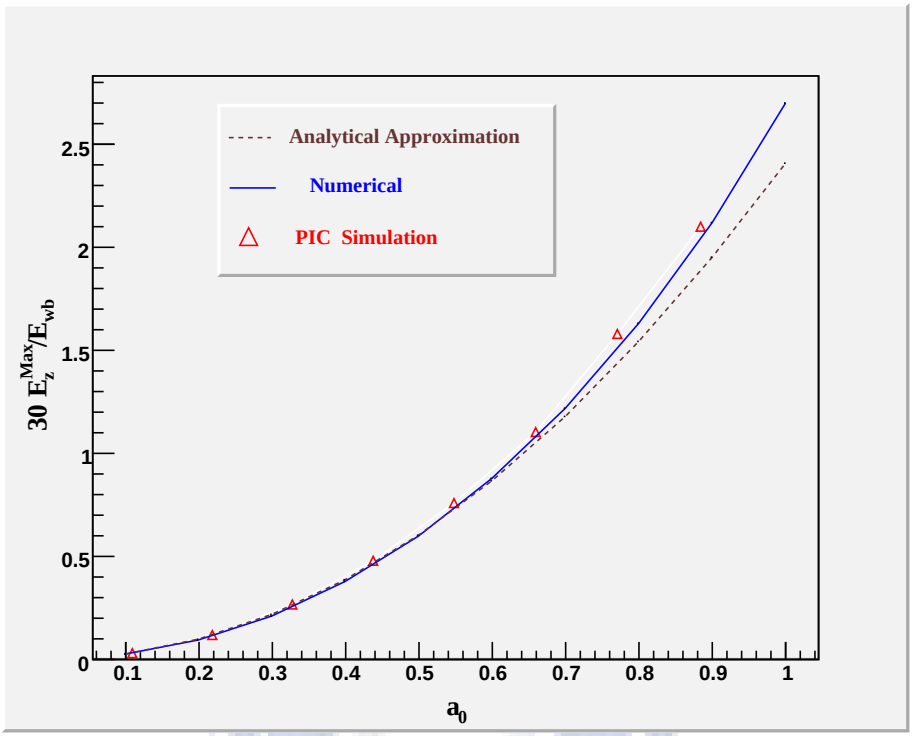

Figure 4.2: This is the comparison of numerical solution with analytical approximation (equation (4.20)) and PIC simulation. The x-axis is the amplitude of the pulse. Other settings of the pulse are $k = \pi\omega_p/c$, $\omega \simeq 3\omega_p$, $\sigma = \frac{8c}{3\sqrt{2}\omega_p}$. The setting of the external magnetic field is $\tilde{B}_0 = 12$.

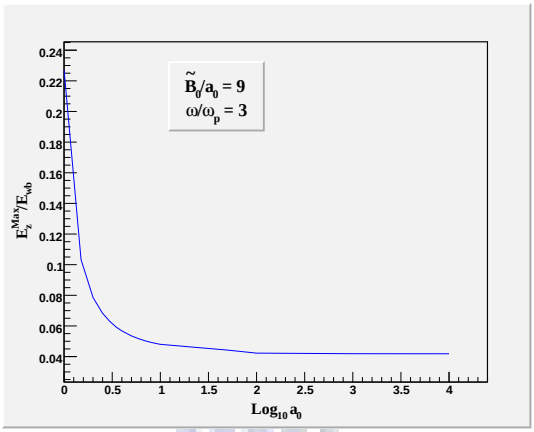

Figure 4.3: The plot of E_z^{Max} for wakefield induced by whistler wave. We fix $\omega/\omega_p = 3$ and $\tilde{B}_0/a_0 = 9$, and increase both a_0 and $\tilde{B}_0$. The Gaussian width of the pulse is $\sigma = 3c/\omega_p$.

We note that these differential equations are derived without any approximation. They are also applicable to the current case.

Comparison with analytical approximation and PIC simulation

We set the pulse as $\mathbf{E} = \mathbf{E}_0 \mathbf{e}^{-i(kz-\omega t)}$, where $\mathbf{E}_0(z,t)$ is taken to be a Gaussian shape. Here the driving pulse is whistler pulse of which the frequency is smaller than the cyclotron frequency. Other settings of the pulse are $kc/\omega_p = \pi$, and the Gaussian width of the pulse $\sigma = \frac{8c}{3\sqrt{2}\omega_p}$. We denote the external magnetic field as B_0, which can be normalized as $\tilde{B}_0 = eB_0/mc\omega_p$.

In Fig. 4.2, we show the comparison of wakefield obtained by different methods. One can see that the numerical solution agrees well with theoretical approximation (equation (4.20)) and "Particle In Cell"(PIC) simulation in the weak field limit. As the amplitude gradually increases, the analytical approximation fails. In other words, the relativistic effect becomes non-negligible.

Having checked the numerical result in the weak field limit, we like to study the behavior of wakefield in the strong field limit. It is to be noted that, if we simply fix the frequency of the pulse and the external magnetic field while verifying the amplitude a_0 of the pulse, the driving pulse would not always stay as the whistler wave. The wave could become R wave when $a_0 >> 1$.

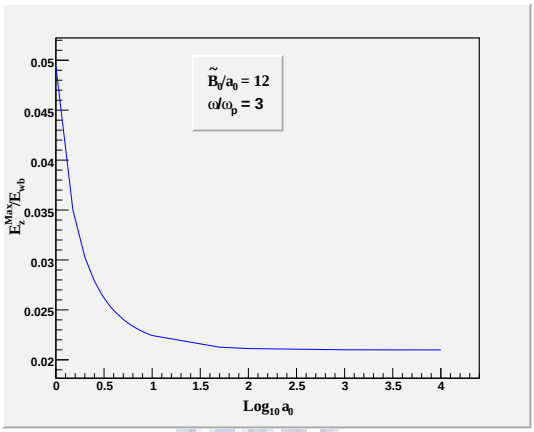

Figure 4.4: The plot of E_z^{Max} for wakefield induced by whistler wave. We fix $\omega/\omega_p = 3$ and $\tilde{B}_0/a_0 = 12$, and increase both a_0 and $\tilde{B}_0$. The Gaussian width of the pulse is $\sigma = 3c/\omega_p$.

To ensure that the driving pulse is a whistler wave, we fix the ratio of the external magnetic field to the amplitude of the pulse while allowing both of them to grow. In Fig. 4.3, we fix $\omega = 3\omega_p$ and $\tilde{B}_0/a_0 = 9$ while in Fig. 4.4 we fix $\omega = 3\omega_p$ and $\tilde{B}_0/a_0 = 12$. Under this settings, we find that the maximum value of the wakefield approaches to certain value as $a_0 >> 1$. We note that the asymptotic value becomes smaller when the ratio of the external magnetic field to the amplitude of the pulse becomes larger.

4.4 Numerical Solution of Wakefield Induced by R Wave

In this section, we analyze the wakefield induced by the R wave, which is seen to be the upper branch shown in Fig. 4.1.

In the last section, we need to increase both the amplitude of the pulse and the external magnetic field to keep the driving pulse in the whistler branch. In this section, we fix the external magnetic field and increase the amplitude of the pulse. The frequency of the pulse remains larger than the cyclotron frequency in this process. Hence the pulse stays as a R wave in the magnetized plasma when we increase the amplitude of the pulse.

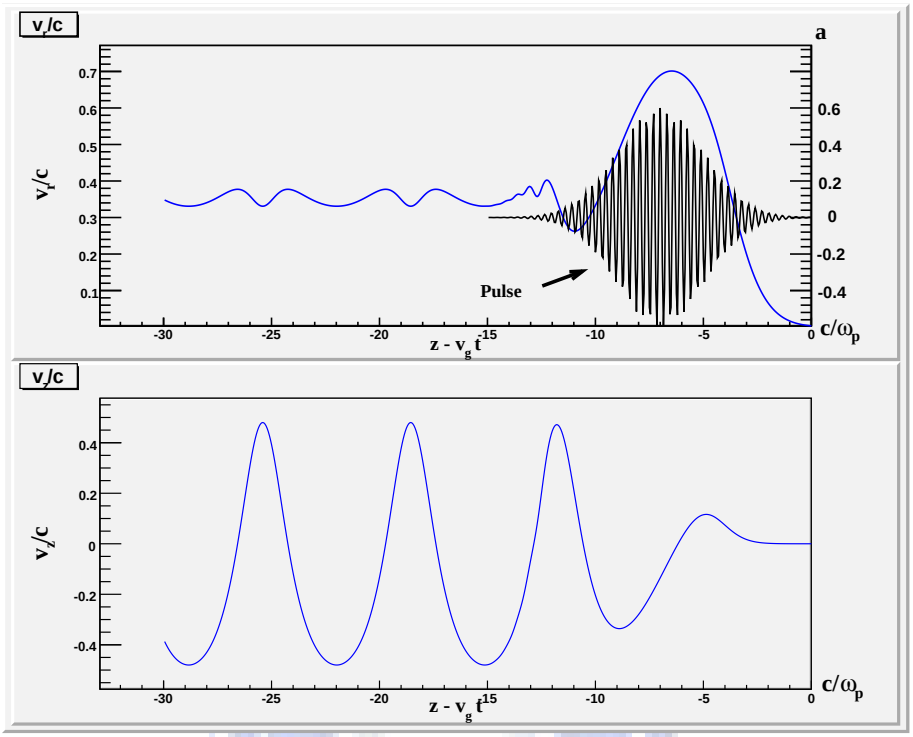

Figure 4.5: This is the plot of velocities of electrons at different positions. The upper graph is v_r and the lower graph is v_z, where $v_r = \sqrt{v_x^2 + v_y^2}$. We set $\tilde{B}_0 = 12$. The settings of the driven pulse are $a_0 = 0.6$ and $\omega/\omega_p = 20$, the Gaussian width is $\sigma = 3c\omega_p$.

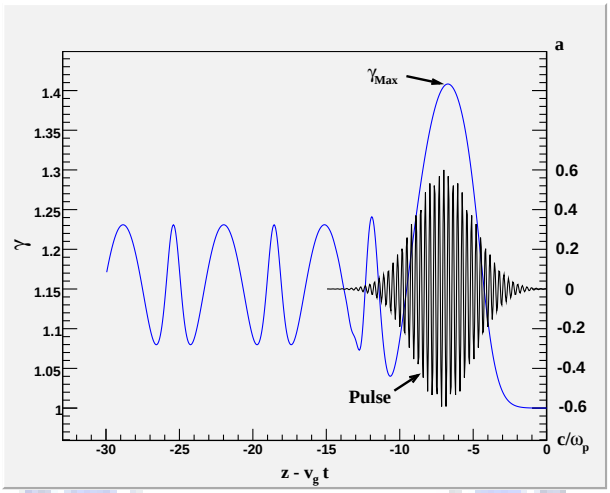

Figure 4.6: The plot of γ factor of electrons at different positions, where $\gamma = 1/\sqrt{1-(|\mathbf{v}|^2/c)}$. All settings of parameters in this plot are the same as Fig. 4.5.

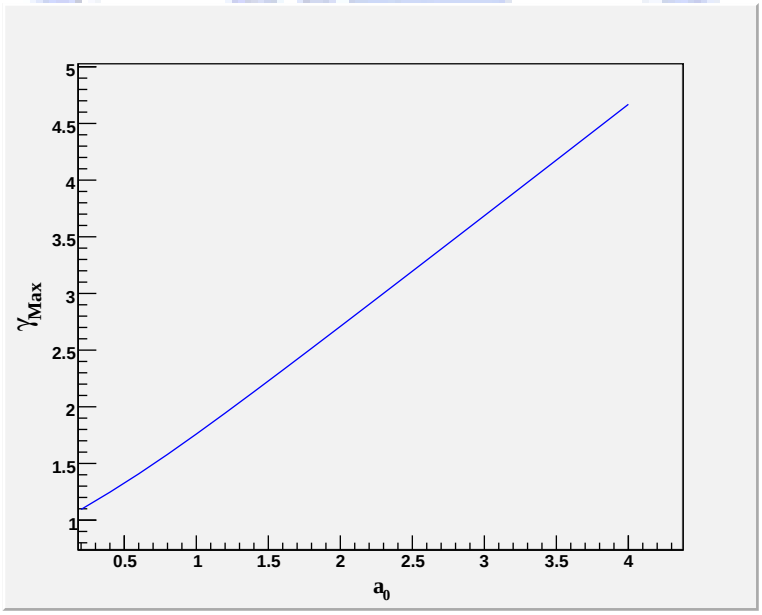

Figure 4.7: The plot of the maximum value of γ versus a_0.

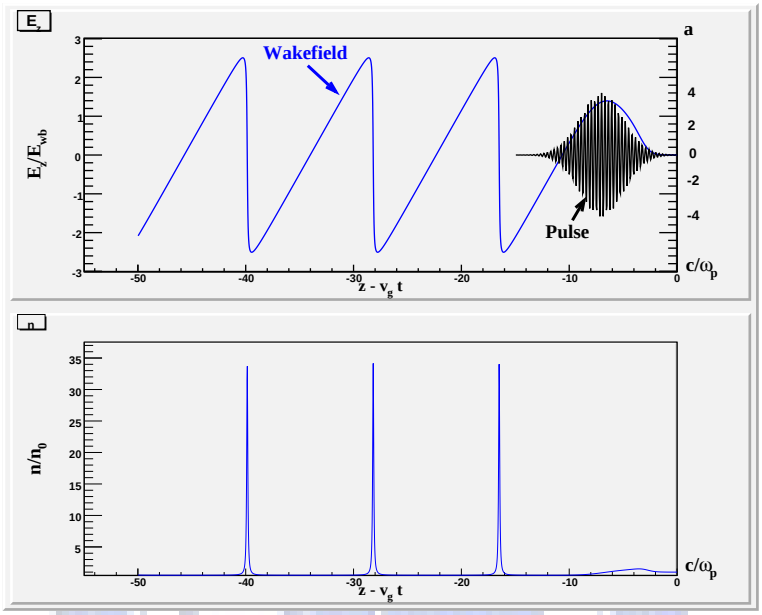

Figure 4.8: The plot of wakefield in the co-moving frame. The settings of the driven pulse are $a_0 = 4, \omega/\omega_p = 20$ and $\sigma = 2c/\omega_p$. The external magnetic field is $\tilde{B}_0 = 12$.

γ factor

For the wakefield induced by R wave, it is desirable to know when we need to consider relativistic motion of the driven electrons. Thus we focus on the value of γ factors of driven electrons, where $\gamma = 1/\sqrt{1 - |\mathbf{v}|^2/c^2}$.

Fig. 4.5 are plots of electron velocities in different positions. We present $v_r = \sqrt{v_x^2 + v_y^2}$ rather than v_x, v_y because electrons are in cyclotron motions around the uniform magnetic field. Therefore, v_x and v_y oscillate in time and v_r is more suitable for presenting the transverse motions of the electrons. From the velocities of electrons, we calculate γ factors of the electrons in different positions (Fig. 4.6). Taking the maximum value of γ factors of electrons driven by the pulse, we show the relation between γ_{Max} and a_0. In Fig 4.7, one can see the maximum value of γ (γ_{Max}) increases linearly with a_0.

Wakefield

We present the wakefield in Fig. 4.8. One can see the saw-tooth-like shape again in the plot which is similar to Fig. 3.1. For larger values of a_0,

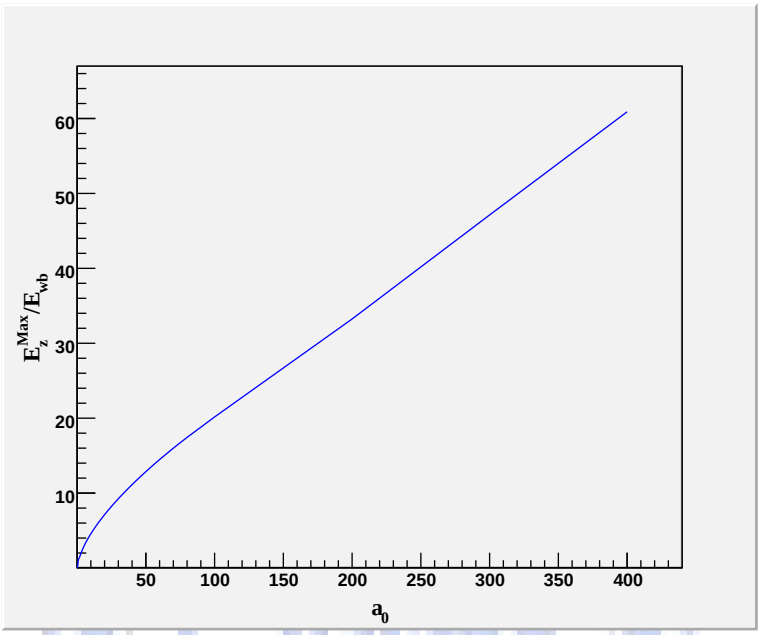

Figure 4.9: The plot of maximum value of wakefield versus a_0 in magnetized plasma. The parameter settings are $\omega/\omega_p = 20, \tilde{B}_0 = 12, \sigma = 2c/\omega_p$.

we find that the relation between E_z^{Max} and a_0 is different from that in the non-magnetized plasma case (Fig. 4.9).

In Fig. 4.9, we find that the growing rate of E_z^{Max} reduces with a_0 when $a_0 < 50$ but remains constant when a_0 becomes larger.

Chapter 5

Conclusion

First of all, we have found that the maximum value of γ factors of the driven electrons increase linearly with a_0 in the magnetized plasma (Fig. 4.5). According to this result, we expect there exists a simple relation between γ and a_0 in the magnetized case.

Secondly, the plot of wakefield in the magnetized plasma (Fig. 4.8) is similar to that in the non-magnetized plasma (Fig. 3.1). For wakefield induced by the strong field pulse, we see the saw-tooth-like shape of wakefiled in both non-magnetized case (Fig. 3.1) and magnetized case (Fig. 4.8). This is because the uniform magnetic background does not affect the longitudinal motions of the electrons. Therefore, the longitudinal waves in two different cases have similar behavior.

Another interesting result is the relation between E_z^{Max} and a_0. If we keep the driving pulse as the whistler pulse and increase both amplitudes of the pulse and the external magnetic field, we find E_z^{Max} approaches to a certain value for $a_0 >> 1$. This asymptotic value is smaller when the ratio of the external magnetic field to the amplitude of the pulse is larger.

Finally, for wakefield driven by the R wave, we find that E_z^{Max} grows linearly with a_0 for a sufficiently larger $a_0 < 50$.

Although numerical solutions work well as seen from many comparisons, there are still some limitations. First of all, we did not consider the dispersion effect of the pulse. Since the pulse is not made of single wave length in reality, it shall disperse in the plasma according to dispersion relation. However, in our numerical analysis, we simply assume the pulse is solid. Secondly, we did not consider the feed back effect of electrons to the pulse. This can only

be taken into account in a self-consistent plasma simulations.

Appendix A

Derivation of Equation (3.11)

First of all, we focus on the z component of the Lorentz force,

$$\frac{dP_z}{dt} = -e(E_z + \frac{1}{c}(v_x B_y - v_y B_x)). \tag{A.1}$$

From Maxwell equations, we have

$$\begin{cases} E_z = -\frac{\partial \Phi}{\partial z} - \frac{\partial A_z}{c\partial t}, \\ \mathbf{B} = \nabla \times \mathbf{A}. \end{cases} \tag{A.2}$$

Let us rewrite equation (A.1)

$$\frac{dP_z}{dt} = -e(-\frac{\partial \Phi}{\partial z} + -\frac{\partial A_z}{c\partial t}\frac{1}{c}(v_x \frac{\partial A_x}{\partial z} + v_y \frac{\partial A_y}{\partial z})). \tag{A.3}$$

With $d/dt = \partial/\partial t + v_z \partial/\partial z$, we change the left hand side of equation (A.2) such that

$$\frac{\partial P_z}{\partial t} + v_z \frac{\partial P_z}{\partial z} = -e(-\frac{\partial \Phi}{\partial z} + -\frac{\partial A_z}{c\partial t}\frac{1}{c}(v_x \frac{\partial A_x}{\partial z} + v_y \frac{\partial A_y}{\partial z})). \tag{A.4}$$

Using the relation between (A_x, A_y) and (P_x, P_y) from equation (2.10), we have

$$\frac{\partial P_z}{\partial t} + v_z \frac{\partial P_z}{\partial z} = -e(-\frac{\partial \Phi}{\partial z} + \frac{e\partial}{2\gamma m c^2 \partial z}|\mathbf{A}|^2), \tag{A.5}$$

where $\gamma = 1/\sqrt{1 - |\mathbf{v}|^2/c^2}$. Changing coordinates

$$\begin{aligned} \xi &= z - v_g t, \\ \tau &= t. \end{aligned} \tag{A.6}$$

Equation (A.5) becomes

$$\frac{\partial}{\partial \xi}[\gamma(1 - \beta_g \beta_z) - \phi] = -\frac{1}{c}\frac{\partial}{\partial \tau}(\gamma \beta_z), \tag{A.7}$$

where $\beta_g = v_g/c$ and $\beta_z = v_z/c$.

Besides the electron equation of motion, we have Poisson equation and continuity equation

$$\nabla^2\Phi = -4\pi e(n - n_0), \tag{A.8}$$

$$\frac{\partial n}{\partial t} + \nabla(n\mathbf{v}) = 0. \tag{A.9}$$

With new coordinates (ξ, τ), we have

$$\frac{\partial^2\phi}{\partial\xi^2} = -\beta_g^2(\frac{n}{n_0} - 1), \tag{A.10}$$

$$\frac{\partial n}{k_p\partial\tau} - \frac{\partial}{\partial\xi}(n(\beta_g - \beta_z)) = 0, \tag{A.11}$$

where $k_p = \omega_p/v_g$.

Quasistatic approximation

Integrate ξ on both side of equation (A.11), we have

$$\int_\xi^\infty \frac{\partial n}{k_p\partial\tau} - \frac{\partial}{\partial\xi'}(n(\beta_g - \beta_z))d\xi' = 0. \tag{A.12}$$

However, when $\xi > 0$ (see Fig 2.1), β_z is zero and n is equal to n_0. Therefore, equation (A.12) can be written as

$$\int_\xi^0 \frac{\partial n}{k_p\partial\tau}d\xi - (n(\beta_g - \beta_z))|_\xi^\infty = 0. \tag{A.13}$$

Furthermore, the first term on the left hand side is very small if $\omega >> \omega_p$. That is, if the frequency of the pulse is very large, the growth rate of density is very small. Therefore, we could drop out the first term of equation (A.12). Hence

$$\begin{aligned} &-(n(\beta_g - \beta_z))|_\xi^\infty = 0 \\ \Rightarrow\quad &-n_0 + n(\xi)\beta_g - n(\xi)\beta_z = 0. \end{aligned} \tag{A.14}$$

Similarly, equation (A.6) could also be written as

$$\gamma(1 - \beta_g\beta_z) - \phi = 1. \tag{A.15}$$

Combining equation (A.10), (A.14), (A.15), we finally have

$$\frac{\partial^2\phi}{\partial\xi^2} = \frac{1}{2}(\frac{1 + |\mathbf{a}|^2}{(1+\phi)^2} - 1). \tag{A.16}$$

Appendix B

Derivation of Equation (4.4)

Let us begin with the electron equation of motion

$$m\frac{d\mathbf{v}}{dt} = -e(\mathbf{E} + (\mathbf{v} \times \mathbf{B})/c). \tag{B.1}$$

In the x and y component form:

$$\begin{cases} m\dfrac{dv_x}{dt} = -e(E_x + (v_y B_z - v_z B_y)/c), \\ m\dfrac{dv_y}{dt} = -e(E_y + (v_z B_x - v_x B_z)/c). \end{cases} \tag{B.2}$$

Recall that B_z is strong uniform magnetic field and B_x, B_y are just induced by the E field. Besides, we assume v_z is much smaller than v_x, v_y here. Hence we may ignore the terms $v_z B_y$ and $v_z B_x$ on the right hand side of equation (B.2). Then we have

$$\begin{cases} \dfrac{dv_x}{dt} = -\dfrac{e}{m}E_x - v_y\omega_c, \\ \dfrac{dv_y}{dt} = -\dfrac{e}{m}E_y + v_x\omega_c. \end{cases} \tag{B.3}$$

where $\omega_c = eB_z/mc$ is the cyclotron frequency.

Defining $\bar{v} = v_x + iv_y$, $\bar{E} = E_x + iE_y$, we can combine the above two equations

$$\frac{d\bar{v}}{dt} = -\frac{e}{m}\bar{E} + i\omega_c\bar{v}. \tag{B.4}$$

For right-handed circularly polarized pulse,

$$\bar{E} = E_x + iE_y = E_0\mathbf{e}^{-i(kz-\omega t)}, \tag{B.5}$$

where E_0 is the amplitude of the pulse, which is a function of z and t.

Therefore, $\bar{v}$ can be solved as

$$\bar{v}(z,t_0)\mathbf{e}^{-i\omega_c t_0} = -\frac{e}{m}\int_{t_0}^{\infty} dt\bar{E}e^{-i\omega_c t} = -\frac{e}{m}\int_{t_0}^{\infty} dtE_0\mathbf{e}^{-ikz+i(\omega-\omega_c)t}. \quad \text{(B.6)}$$

Using integration by part, we arrive at

$$\bar{v}(z,t_0)\mathbf{e}^{-i\omega_c t_0} = -\frac{e}{m}\frac{1}{i(\omega-\omega_c)}[E_0\mathbf{e}^{-ikz+i(\omega-\omega_c)t}|_{t_0}^{\infty} - \int_{t_0}^{\infty} dt\dot{E}_0\mathbf{e}^{-ikz+i(\omega-\omega_c)t}], \quad \text{(B.7)}$$

where $\dot{E}_0 = dE_0/dt$. For the first term on the right hand side, the value of E_0 vanishes as t goes to infinity. For the second term, we perform integration by part again

$$\begin{aligned}\bar{v}(z,t_0)\mathbf{e}^{-i\omega_c t_0} = & -\tfrac{e}{m}\tfrac{1}{i(\omega-\omega_c)}[E_0\mathbf{e}^{-ikz+i(\omega-\omega_c)t_0} - \tfrac{1}{i(\omega-\omega_c)}[\dot{E}_0\mathbf{e}^{-ikz+i(\omega-\omega_c)t}|_{t_0}^{\infty} \\ & - \textstyle\int_{t_0}^{\infty} dt\ddot{E}_0\mathbf{e}^{-ikz+i(\omega-\omega_c)t}]],\end{aligned} \quad \text{(B.8)}$$

where $\ddot{E}_0 = d^2E_0/dt^2$. Since $E_0(z,t)$ represents the amplitude of the pulse, the second derivative term $\ddot{E}_0$ must be much smaller than $(\omega-\omega_c)$. This is because the former represent the slow variation of the amplitude while the later represent the fast oscillation. Hence we can ignore the third term on the right hand side.

Assuming $\dot{E}_0$ is zero as t goes to infinity we conclude

$$\bar{v}(z,t) = -\frac{e}{m}\frac{1}{i(\omega-\omega_c)}(E_0\mathbf{e}^{-ikz+i\omega t} - \frac{1}{i(\omega-\omega_c)}\dot{E}_0\mathbf{e}^{-ikz+i\omega t}). \quad \text{(B.9)}$$

From the Maxwell equation

$$\nabla\times\mathbf{E} = -\frac{1}{c}\frac{\partial\mathbf{B}}{\partial t}, \quad \text{(B.10)}$$

we have

$$\bar{B} = B_x + iB_y = -\frac{c}{\omega}(\frac{\partial E_0}{\partial z}\mathbf{e}^{-i(kz-\omega t)} - ikE_0\mathbf{e}^{-i(kz-\omega t)} + i\frac{1}{\omega}\frac{\partial\dot{E}_0}{\partial z}\mathbf{e}^{-i(kz-\omega t)} + \frac{k}{\omega}\dot{E}_0\mathbf{e}^{-i(kz-\omega t)}). \quad \text{(B.11)}$$

In equation (4.3), we have defined

$$f_{\parallel} = \frac{-e}{c}(v_xB_y - v_yB_x). \quad \text{(B.12)}$$

Hence, by combining equation (B.9) and (B.11), we obtain

$$f_{\parallel} = \frac{e^2}{m\omega(\omega-\omega_c)}(-E_0\frac{\partial E_0}{\partial z} - \frac{k}{\omega}E_0\dot{E}_0 + \frac{k}{\omega-\omega_c}E_0\dot{E}_0 - \frac{1}{\omega(\omega-\omega_c)}\dot{E}_0\frac{\partial \dot{E}_0}{\partial z}). \tag{B.13}$$

Again, the fourth term on the right hand side is very small since the second derivative term $\partial\dot{E}_0/\partial z$ is negligible compare to $(\omega-\omega_c)$. Therefore, we finally have

$$f_{\parallel} = \frac{-1}{2}(\frac{\partial}{\partial z} - \frac{k\omega_c}{\omega(\omega-\omega_c)}\frac{\partial}{\partial t})\frac{e^2E_0^2}{m\omega(\omega-\omega_c)}. \tag{B.14}$$

Bibliography

[1] Pierre- Alain Duc, et al. arXiv: astro- ph/ 0408524v1.

[2] E.Fermi, Phys. Rev. 75, 1169 (1949)

[3] S. C. Corbato et al., Nucl. Phys. B(Proc. Suppl.) **28B**, 36 (1992)

[4] R. Knapik et al. (Auger Coll.), arXiv: 0708.1924; presented at 30th Int. Cosmic Ray Conf. (ICRC), 2007.

[5] K. Greisen, Phys. Rev. Lett. **16** (1966) 748

[6] G. T. Zatepin and V. A. Kuz'min, Sov. Phys. JETP. Lett. 4 (1966) 78

[7] T.Tajima, J.M.Dawson, Phys. Rev. Lett. 43 267 (1979)

[8] P.Chen, T.Tajima and Y.Takahashi, Phys. Rev. Lett. 89 161101 (2002)

[9] F-Y.Chang et al.,arXiv: 0709.1177

[10] E.Esarey, et al.,IEEE Trans. Plasma Sci: 24 (1996)

[11] L.M.Gorbunov and V.I.Kirsanov, Zh Eksp. Teor. Fiz. 93, 509 (1987) [Sov. Phys. - JETP 66, 290 (1987)]

[12] P.Sprangle, E.Esarey, and A.Ting, "Nonlinear theory of intense laser pulses in plasma", Phys. Rev. A, vol. 41, pp. 4463-4469 ,1990.

[13] H.Washimi and V.I.Karpman, JETP 71, 1010 (1976)

[14] M. Marklund, P. K. Shukla, L. Stenflo, G. Brodin and M. Servin. Plasma Phys. Control. Fusion **47** (2005) L25-L29

[15] V. I. Berezhiani and I. G. Murusidze. Physica Scripta. Vol. 45, 87-90, 1992.